Journal of Nuclear Science and Technology

ISSN: 0022-3131 (Print) 1881-1248 (Online) Journal homepage: http://www.tandfonline.com/loi/tnst20

Simplified Treatments of Anisotropic Scattering in LWR Core Calculations

Akio YAMAMOTO , Yasunori KITAMURA & Yoshihiro YAMANE

To cite this article: Akio YAMAMOTO , Yasunori KITAMURA & Yoshihiro YAMANE (2008) Simplified Treatments of Anisotropic Scattering in LWR Core Calculations, Journal of Nuclear Science and Technology, 45:3, 217-229

To link to this article: http://dx.doi.org/10.1080/18811248.2008.9711430

Journal of NUCLEAR SCIENCE and TECHNOLOGY, Vol. 45, No. 3, p. 217–229 (2008)

ARTICLE

Simplified Treatments of Anisotropic Scattering in LWR Core Calculations

Akio YAMAMOTO, Yasunori KITAMURA and Yoshihiro YAMANE

Department of Materials, Physics and Energy Engineering, Nagoya University, Furo-cho, Chikusa-ku, Nagoya 464-8603, Japan

(Received August 28, 2007 and accepted in revised form November 15, 2007)

The validity of various simplified treatments of anisotropic scattering is investigated in typical LWR configurations that simulate PWR, BWR, and APWR. In addition to the explicit treatment of anisotropic scattering, the diagonal approximation of anisotropic scattering matrixes and the transport corrected cross section with the assumption of isotropic scattering are also tested. Calculation results indicate that the anisotropic scattering matrix of the P1 component would be explicitly treated to obtain accurate results in the present calculations. The P2 or higher order anisotropic scattering matrix could be approximated by the diagonal approximation while maintaining the calculation accuracy. In addition to the above investigation, the physical meaning of the transport corrected cross section used in a transport calculation is discussed through a simple one-group fixed-source benchmark problem with anisotropic scattering. Though the transport corrected cross section is usually used to consider the P1 scattering cross section, the calculation results and discussion clarify that the transport corrected cross section is not mathematically consistent with the consideration of the P1 scattering cross section. The transport corrected cross section always implicitly includes an infinite order of anisotropic scattering cross sections when it is used in a transport calculation. Since the higher order anisotropic scattering component tends to reduce neutron leakage from a core, the calculated k-effective with the transport corrected cross section would be overestimated. This suggests the cause of the overestimation of k-effective by transport calculation with the transport corrected cross section obtained by in-scatter approximation.

KEYWORDS: anisotropic scattering, transport corrected cross section, transport calculation, out-scatter approximation, in-scatter approximation, LWR

I. Introduction

In the light water reactor analyses, the anisotropy of scattering is generally treated by simplified approximations, *i.e.*, the transport corrected cross section and isotropic scattering approximations, from the viewpoint of computational efficiency. These approximations have been supported by rich experiences in LWR analyses regardless of their simplicity. However, the recent studies suggest that the consideration of higher order anisotropic scattering is important in some situations, *e.g.*, MOX fuel-loaded or high-leakage small cores.[1–4] Therefore, recent advanced neutronics codes gradually take into account the higher order anisotropic scattering.[3–5,7] Especially, the utilization of the method of characteristics (MOC) allows an easy incorporation of the higher order anisotropic scattering in LWR analyses.

However, the incorporation of the higher order anisotropic scattering is generally memory storage intensive since scattering matrixes, which occupy a considerable fraction of memory storage in neutronics calculations, should be retained for higher order anisotropy. When the P3 scattering is taken into account, storage requirement for the scattering matrixes is four times larger than that of the conventional P0 calculation with the transport corrected cross sections. Such a memory requirement would be acceptable for lattice physics calculations, but it would be impractical for larger configurations, *e.g.*, whole core calculations. Therefore, an approximate treatment of anisotropic scattering is desirable in the production calculations.

There are two major issues for the treatment of anisotropic scattering. The first one is related to the generation of the multigroup total cross sections. In the transport equation, the total cross section is multiplied by the angular flux. Therefore, the collapsed (*i.e.*, multigroup) total cross section should have angular dependency. However, common transport codes do not have the capability to treat the angular-dependent total cross sections. Thus, several simplifications (*e.g.*, the consistent-P or the extended transport correction) are widely used to handle this issue.[8] The angular dependence of the total cross section is approximately taken into account as the correction term of the diagonal element of an anisotropic scattering matrix. Therefore, the above simplification has impact on the (multigroup) anisotropic scattering matrix. This problem is well discussed in some references.[8–10]

Once the multigroup cross sections with anisotropic scattering are derived, we commonly perform further approxi-

mation on this cross section set. Since a transport calculation with anisotropic scattering is time consuming and memory intensive, isotropic scattering is favored over the rigorous treatment of anisotropic scattering in common LWR analyses. Furthermore, since diffusion calculation is historically used in the LWR core analysis, isotropic scattering is desirable. This simplification (isotropic approximation) is the second issue for the treatment of anisotropic scattering. As described previously, the transport correction is commonly used to resolve this issue.

This paper focuses on the second issue. Namely, we assume that the multigroup cross section with anisotropic scattering is "given" and a transport calculation with the "given" anisotropic scattering is considered as the reference solution in the present study. Discussion on the first issue, *i.e.*, the treatment of the angular-dependent total cross section, is beyond the scope of this paper.

The contributions of this paper are summarized as follows:

(1) Estimate accuracies of various simplified treatments of anisotropic scattering in typical LWR configurations. Various fuel types (UO_2, MOX) and reflector types (PWR, BWR, APWR) are taken into account.

There are several studies that discuss the impact of transport corrected cross sections.[1,2,4,8,9,12] However, systematic investigation on the simplified treatments of the anisotropic scattering has not been carried out in an LWR configuration to the best of the authors' knowledge.

(2) Discuss the physical meaning of the transport corrected cross section in a transport calculation.

The utilization of the transport corrected cross section shows discrepancy from the reference results with an explicit treatment of anisotropic scattering. In order to resolve this issue, the physical meaning of the transport corrected cross section in a transport calculation is discussed. The authors believe that the interpretation of the transport corrected cross section in a transport calculation has not been carried out so far.

The rest part of the paper is organized as follows. In section II, various simplified treatments of anisotropic scattering, which are tested in the present study, are described. In section III, procedures of numerical calculations and results are given. Discussions on the transport corrected cross section are presented in section IV. Finally, concluding remarks are summarized in section V.

II. Simplified Treatments of Anisotropic Scattering

As described in Introduction, the multigroup cross section with an anisotropic scattering matrix is given in the present study. The maximum order of the anisotropic scattering matrix is assumed to be P3 based on the results of previous studies.[1,2] A more detailed explanation about the calculation condition will be given in section III.

In order to investigate the impact of an anisotropic scattering treatment, various simplifications are tested in the present study as follows.

- P1
- P2
- P3
- Tr
- P0-P1
- P0-P2
- P0-P3
- P1-P2
- P1-P3
- P2-P3

The detailed descriptions on these treatments are given below:

P1: Scattering matrixes up to the P1 component are explicitly taken into account. The P2 and P3 components are neglected.

P2: Scattering matrixes up to the P2 component are explicitly taken into account. The P3 component is neglected.

P3: Scattering matrixes up to the P3 component are explicitly taken into account. The obtained result is taken as the reference solution in the present study.

Transport corrected cross section (Tr): The transport corrected cross section is used to approximately consider the anisotropic scattering.

In the transport corrected cross section, though the P1 component is approximately taken into account, the P2 and P3 components are neglected. With the transport corrected cross section, only isotropic scattering (P0 component) is explicitly used in the calculation. Though various transport corrected cross sections can be used,[8,9] the definition of the transport corrected cross section can be written as

$$\Sigma_{tr,g} = \Sigma_{t,g} - \frac{\sum_{g'} \Sigma_{s1,g' \to g} \phi_{1,g'}}{\phi_{1,g}}, \tag{1}$$

where

$\Sigma_{tr,g}$: transport corrected cross section of g-th energy group,

$\Sigma_{t,g}$: total cross section of g-th energy group,

$\Sigma_{s1,g' \to g}$: P1 scattering cross section from g'-th to g-th energy group, and

$\phi_{1,g}$: P1 component of angular flux, *i.e.*, neutron current.

Unfortunately, an accurate evaluation of the P1 component of angular flux is impractical since a detailed transport calculation is necessary prior to the evaluation of the transport corrected cross section. Therefore, in the present study, two different approximations are used for the P1 component of angular flux. In the first case, the typical total (P0) flux $\phi_{0,g}$ is approximately used for $\phi_{1,g}$. Note that cell average flux for typical UO_2 fuel in PWR (^{235}U enrichment: 4.1 wt%) is used for $\phi_{0,g}$. There are two reasons for this simplified treatment. The first reason is that this treatment would be justified since the spatial flux distribution is flat in the high-energy region in which the effect of the transport corrected cross section is large. The second reason is that this treatment is practical in actual in-core fuel management calculations. In principle, the position- and group-dependent flux ($\phi_{0,g}$) can be obtained by detailed anisotropic transport calculation in a core configuration including a reflector region. However, in actual in-core fuel management calculations, such detailed calculation would be prohibitive for the evaluation of the transport cross section from the view-

point of computation time. Therefore, a position-independent (*i.e.*, typical) neutron spectrum is used in the present study from the practical point of view. In other words, the potential discrepancy caused by the above simplified treatment is included in the accuracy estimation of the present study.

In this case, the transport corrected cross section is evaluated using

$$\Sigma_{tr,g} = \Sigma_{t,g} - \frac{\sum_{g'} \Sigma_{s1,g'\to g}\phi_{0,g'}}{\phi_{0,g}}. \quad (2)$$

In the second case, the following approximation is used to evaluate $\phi_{1,g}$:[9,11]

$$\phi_{1,g} \approx \frac{\phi_{0,g}}{\Sigma_{t,g}}. \quad (3)$$

Thus, the transport corrected cross section is evaluated using

$$\Sigma_{tr,g} = \Sigma_{t,g} - \frac{\sum_{g'} \Sigma_{s1,g'\to g}(\phi_{0,g'}/\Sigma_{t,g'})}{(\phi_{0,g}/\Sigma_{t,g})}. \quad (4)$$

Equation (1) can be further simplified by assuming that

$$\sum_{g'} \Sigma_{s1,g'\to g}\phi_{1,g'} \approx \sum_{g'} \Sigma_{s1,g\to g'}\phi_{1,g}$$

with the result that

$$\Sigma_{tr,g} = \Sigma_{t,g} - \sum_{g'} \Sigma_{s1,g\to g'}. \quad (5)$$

Equations (1) and (5) are called the in-scatter and out-scatter approximations, respectively. Therefore, Eqs. (2) and (4) are the variants of the in-scatter approximation. To sum up, there are three variations for the derivation of the transport corrected cross section in this study:

- the in-scatter approximation with scalar flux as a weighting function, *i.e.*, Eq. (2),
- the in-scatter approximation with the approximated current as a weighting function, *i.e.*, Eq. (4), and
- the out-scatter approximation, *i.e.*, Eq. (5).

It should be noted that the above three variations for the transport corrected cross section are applied to the energy range higher than 1 keV and that the out-scatter approximation is always used for the energy range lower than 1 keV.

This treatment would be justified by the fact that the transport corrected cross sections obtained by the in-scatter and out-scatter approximations well agree with each other at most energy ranges lower than 1 keV, as will be shown in section III. This suggests that the detailed energy balance for the P1-slowing down source used during the derivation of Eq. (5) is well established for most energy ranges lower than 1 keV. However, it should be noted that the difference between the in-scatter and out-scatter approximations becomes larger in some energy groups in which resonance peaks of ^{238}U exist. In these energy groups, the transport corrected cross section obtained by the in-scatter approximation may be negative. Since the negative transport cross section can be a cause of a numerical problem as will be discussed in detail in section III, only the out-scatter approximation is applied to the energy range lower than 1 keV in the present study.

P0-P1: The P0 scattering matrix is treated as is. The P1 scattering matrix is approximated only using the diagonal element, and the off-diagonal elements of the P1 scattering matrix are set to be zero. The P2 and P3 components are neglected. The diagonal element of the P1 component is evaluated by the following three different ways.

$$\Sigma_{s1,g\to g} \approx \frac{\sum_{g'} \Sigma_{s1,g'\to g}\phi_{0,g'}}{\phi_{0,g}} \quad \text{(in-scatter with P0 flux weight)} \quad (6)$$

$$\Sigma_{s1,g\to g} \approx \frac{\sum_{g'} \Sigma_{s1,g'\to g}\phi_{1,g'}}{\phi_{1,g}} \quad \text{(in-scatter with P1 flux weight)} \quad (7)$$

$$\Sigma_{s1,g\to g} \approx \sum_{g'} \Sigma_{s1,g\to g'} \quad \text{(out-scatter)} \quad (8)$$

The P1 flux, *i.e.*, $\phi_{1,g}$, is evaluated using formula (3). The P2 and P3 components are neglected.

In this approach, only the diagonal element of the P1 matrix should be retained during calculations. Therefore, the memory requirement for the scattering matrix can be reduced compared with the "P1" treatment that utilizes the full P1 scattering matrix.

P0-P2: The P0 scattering matrix is treated as is. The P1 and P2 scattering matrixes are approximated using the diagonal elements. The off-diagonal elements of the P1 and P2 scattering matrixes are set to be zero. The diagonal elements of the P1 scattering matrix are evaluated by the same approach of "P0-P1" (*i.e.*, formulae (6)–(8)), and those of the P2 scattering matrix are evaluated by the following approximations.

$$\Sigma_{s2,g\to g} \approx \frac{\sum_{g'} \Sigma_{s2,g'\to g}\phi_{0,g'}}{\phi_{0,g}} \quad \text{(in-scatter with P0 flux weight)} \quad (9)$$

$$\Sigma_{s2,g\to g} \approx \frac{\sum_{g'} \Sigma_{s2,g'\to g}\phi_{2,g'}}{\phi_{2,g}} \quad \text{(in-scatter with P2 flux weight)} \quad (10)$$

$$\Sigma_{s2,g\to g} \approx \sum_{g'} \Sigma_{s2,g\to g'} \quad \text{(out-scatter)} \quad (11)$$

Note that the P2 component of the angular flux is approximated using

$$\phi_{2,g} \approx \frac{\phi_{0,g}}{(\Sigma_{t,g})^2}. \quad (12)$$

The P3 component is neglected.

P0-P3: The P0 scattering matrix is treated as is. The P1, P2, and P3 scattering matrixes are approximated using the diagonal elements. The off-diagonal elements of the P1, P2, and P3 scattering matrixes are set to be zero. The diagonal ele-

ments of the P1 and P2 scattering matrixes are evaluated by the same approach used for "P0-P2" (*i.e.*, formulae (6)–(11)), and those of the P3 scattering matrix are evaluated by the following approximations.

$$\Sigma_{s3,g\to g} \approx \frac{\sum_{g'} \Sigma_{s3,g'\to g}\phi_{0,g'}}{\phi_{0,g}} \quad \text{(in-scatter with P0 flux weight)} \tag{13}$$

$$\Sigma_{s3,g\to g} \approx \frac{\sum_{g'} \Sigma_{s3,g'\to g}\phi_{3,g'}}{\phi_{3,g}} \quad \text{(in-scatter with P3 flux weight)} \tag{14}$$

$$\Sigma_{s3,g\to g} \approx \sum_{g'} \Sigma_{s3,g\to g'} \quad \text{(out-scatter)} \tag{15}$$

Note that the P3 component of the angular flux is approximated using

$$\phi_{3,g} \approx \frac{\phi_{0,g}}{(\Sigma_{t,g})^3}. \tag{16}$$

P1-P2: The P0 and P1 scattering matrixes are treated as is. The P2 scattering matrix is approximated using the diagonal elements. The off-diagonal elements of the P2 scattering matrix are set to be zero. The diagonal elements of the P2 scattering matrix are evaluated by the previous approach (*i.e.*, formulae (9)–(11)). The P3 component is neglected.

P1-P3: The P0 and P1 scattering matrixes are treated as is. The P2 and P3 scattering matrixes are approximated using the diagonal elements. The off-diagonal elements of the P2 and P3 scattering matrixes are set to be zero. The diagonal elements of the P2 and P3 scattering matrixes are evaluated by the previous approach (*i.e.*, formulae (9)–(11), (13)–(15)).

P2-P3: The P0, P1, and P2 scattering matrixes are treated as is. The P3 scattering matrix is approximated using the diagonal elements. The off-diagonal elements of the P3 scattering matrix are set to be zero. The diagonal elements of the P3 scattering matrix are evaluated by the previous approach (*i.e.*, formulae (13)–(15)).

III. Numerical Calculations and Discussion

1. Calculation Configurations

Two different calculation configurations, which have different neutron leakage properties, are used to verify the approximate treatments of anisotropic scattering. These are a single pin cell without leakage and a high-leakage small core shown in **Figs. 1** and **2**, respectively. Both configurations are analyzed in two-dimensional geometry. The latter simulates a small critical assembly or an LWR reflector calculation configuration. Since leakage is dominant in the latter configuration, the effect of simplification on the anisotropic scattering will be larger.

The outer radii of the pellet and clad are 0.41 and 0.475 cm, respectively. The cell pitch is assumed to be 1.26 cm. These dimensions are taken from the typical 17 × 17 PWR fuel. The reflective boundary condition is applied to both configurations.

The effect of the anisotropic scattering also depends on the fuel type, as described in Introduction. Therefore, 2.0 wt% UO_2, 4.1 wt% UO_2, and 12 wt% Pu-t MOX fuels are used in the present study. The Pu isotopic composition of the MOX fuel is $^{238}Pu/^{239}Pu/^{240}Pu/^{241}Pu/^{242}Pu/^{241}Am = 2\%/60\%/20\%/10\%/6\%/2\%$. These fuels well cover typical fuel types in major LWRs.

Three different reflectors are used in the small core configuration since the effect of the anisotropic scattering depends on the reflector type. The following reflector types are used.

- Stainless steel (SS) baffle plate whose thickness is 2.52 cm and water
- Bulk water
- Bulk stainless steel (SS)

These reflectors simulate typical PWRs, BWRs, and APWRs (or EPRs), respectively.

2. Calculation Conditions

The calculations are carried out using the AEGIS code, which is a lattice physics code based on MOC and is being developed by Nuclear Engineering, Ltd. with the cooperation of Nagoya University and Nuclear Fuel Industries, Ltd.[13] Cross sections are generated using AELIB, which is a dedicated nuclear data library for the AEGIS code. The major features of AELIB are shown as follows.[14]

- 172 energy groups with the XMAS energy-group structure
- Anisotropic scattering up to the P3 component
- Based on ENDF/B-VI.8

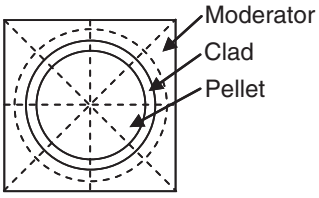

Fig. 1 Pin cell configuration

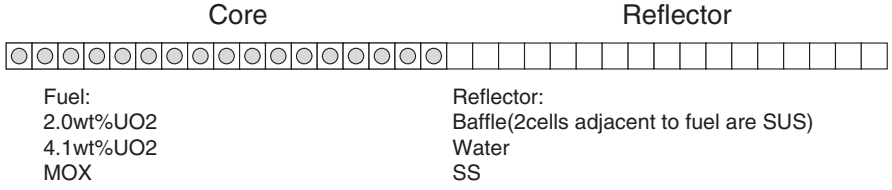

Fig. 2 Small core configuration

Table 1 K-infinity in cell configuration

Method	Treatment of scattering matrix		Evaluation of	K-infinity			Difference (pcm)		
	Full	Diagonal	diagonal element	4.1 wt% UO2	2 wt% UO2	12 wt% MOX	4.1 wt% UO2	2 wt% UO2	12 wt% MOX
P0	P0	—	—	1.37468	1.21986	1.19058	22	14	118
P1	P0, P1	—	—	1.37398	1.21941	1.18807	−29	−23	−93
P2	P0, P1, P2	—	—	1.37448	1.21979	1.18934	8	8	14
P3	P0, P1, P2, P3	—	—	1.37437	1.21969	1.18917	0	0	0
Out-scatter-tr	P0	—	Out-scat.	1.37527	1.22035	1.19218	66	54	253
In-scatter-tr			In-scat., P0 flux wgt	1.37534	1.22043	1.19232	71	61	264
In-scatter-tr			In-scat., PL flux wgt	1.37533	1.22042	1.19230	70	60	263
P0-P1	P0	P1	Out-scat.	1.37310	1.21855	1.18714	−92	−93	−171
			In-scat., P0 flux wgt	1.37310	1.21855	1.18715	−92	−93	−170
			In-scat., PL flux wgt	1.37311	1.21856	1.18715	−92	−93	−170
P0-P2	P0	P1, P2	Out-scat.	1.37390	1.21924	1.18880	−34	−36	−31
			In-scat., P0 flux wgt	1.37391	1.21924	1.18881	−34	−36	−30
			In-scat., PL flux wgt	1.37390	1.21925	1.18881	−34	−36	−31
P0-P3	P0	P1, P2, P3	Out-scat.	1.37391	1.21925	1.18859	−33	−36	−49
			In-scat., P0 flux wgt	1.37391	1.21925	1.18859	−33	−36	−49
			In-scat., PL flux wgt	1.37408	1.21941	1.18910	−21	−22	−6
P1-P2	P0, P1	P2	Out-scat.	1.37477	1.22009	1.18971	29	33	45
			In-scat., P0 flux wgt	1.37477	1.22009	1.18971	29	33	45
			In-scat., PL flux wgt	1.37477	1.22009	1.18971	29	33	45
P1-P3	P0, P1	P2, P3	Out-scat.	1.37478	1.22010	1.18950	30	34	27
			In-scat., P0 flux wgt	1.37477	1.22009	1.18949	29	33	26
			In-scat., PL flux wgt	1.37482	1.22055	1.18999	33	71	69
P2-P3	P0, P1, P2	P3	Out-scat.	1.37449	1.21980	1.18913	9	9	−3
			In-scat., P0 flux wgt	1.37449	1.21979	1.18912	9	9	−4
			In-scat., PL flux wgt	1.37475	1.22006	1.18962	28	31	38

- Ultrafine-energy (32,000) group cross section data for the resolved resonance energy range.

The simplified treatments of the anisotropic scattering described in the previous section are implemented in the cross section processing part of the AEGIS code.

Transport calculations are carried out in 172 energy groups without spatial homogenization, *i.e.*, the calculation geometry is treated as is. Discretization parameters used in the transport calculation using MOC are shown below.

- Number of azimuthal angle divisions (for 2π): 64
- Number of polar angle divisions (for $\pi/2$): 2 (using Tabuchi-Yamamoto's quadrature set[15])
- Width of ray trace: less than 0.1 cm using the macroband method
- Relative convergence criterion for flux and k-effective: 10^{-5}
- Spatial subdivisions of a cell: four annular and eight azimuthal regions, as shown in Fig. 1 (32 flat flux regions in a cell)

The above calculation conditions are used throughout the calculations.

3. Results and Discussion

Calculation results in the pin-cell geometry and differences from the reference (P3) results are shown in **Table 1**. As in the previous studies,[1,2] the transport approximations (both the in-scatter and out-scatter approximations) overestimate k-infinity for all types of fuel. Especially, a positive bias is clearly observed in the high-Pu-content MOX fuels.

Though the P1 results slightly underestimate k-infinity, the P2 results almost reproduce the reference (P3) results. Therefore, P2 anisotropic scattering is sufficient for the fuel types in the present study, which almost cover typical ones used in LWR, under the non-leakage condition.

The P0-P1, P0-P2, and P0-P3 results generally underestimate k-infinity. In the P0-P1 results, the difference between the reference results significantly depends on the fuel type though the P0-P2 and P0-P3 results give similar biases for all fuel types. This observation suggests that the P2 component plays the important role of reducing the fuel-type-dependent bias of k-infinity.

Though the P1-P2 and P1-P3 results show slightly positive biases, variations in these biases are insensitive to the fuel type. Actually, variations in the biases of the P1-P2 and P1-P3 results are comparable to that of P2 and smaller than that of P1. Since P1-P2 and P1-P3 consider diagonal elements of scattering matrixes for P2 and P3, these approximations can reduce the memory storage requirements for scattering matrixes while keeping an accuracy comparable to that of P2. Furthermore, reduction in computation time is also expected since slowing down source calculation for higher order anisotropic scattering requires considerable computation time.

Differences from the reference (P3) results for the small cores are summarized in **Tables 2–4**. In general, the magnitude of discrepancy from the reference results becomes larger than those in the cell calculation since leakage is dominant and the anisotropy of angular flux is larger in the small core configurations. Furthermore, the trend of differences is significantly different from those in the cell configuration.

Table 2 K-effective in small core configuration (SS baffle reflector, PWR)

Method	Treatment of scattering matrix		Evaluation of	K-infinity			Difference (pcm)		
	Full	Diagonal	diagonal element	4.1 wt% UO2	2 wt% UO2	12 wt% MOX	4.1 wt% UO2	2 wt% UO2	12 wt% MOX
P0	P0	—	—	1.23553	1.08562	1.08751	4469	4771	3932
P1	P0, P1	—	—	1.18154	1.03524	1.04471	−95	−91	−159
P2	P0, P1, P2	—	—	1.18282	1.03630	1.04657	12	12	19
P3	P0, P1, P2, P3	—	—	1.18267	1.03618	1.04637	0	0	0
Out-scatter-tr	P0	—	Out-scat.	1.17910	1.03291	1.04463	−302	−316	−166
In-scatter-tr			In-scat., P0 flux wgt	1.19007	1.04270	1.05433	625	629	761
In-scatter-tr			In-scat., PL flux wgt	div.*)	div.	div.	div.	div.	div.
P0-P1	P0	P1	Out-scat.	1.17331	1.02785	1.03690	−791	−804	−905
			In-scat., P0 flux wgt	1.18629	1.03940	1.04840	306	310	194
			In-scat., PL flux wgt	div.	div.	div.	div.	div.	div.
P0-P2	P0	P1, P2	Out-scat.	1.17494	1.02927	1.03917	−654	−667	−688
			In-scat., P0 flux wgt	1.18772	1.04065	1.05049	427	431	394
			In-scat., PL flux wgt	div.	div.	div.	div.	div.	div.
P0-P3	P0	P1, P2, P3	Out-scat.	1.17491	1.02925	1.03895	−656	−669	−708
			In-scat., P0 flux wgt	1.18767	1.04060	1.05024	422	426	370
			In-scat., PL flux wgt	div.	div.	div.	div.	div.	div.
P1-P2	P0, P1	P2	Out-scat.	1.18303	1.03654	1.04686	31	34	47
			In-scat., P0 flux wgt	1.18301	1.03651	1.04683	29	32	44
			In-scat., PL flux wgt	1.18312	1.03661	1.04694	38	41	55
P1-P3	P0, P1	P2, P3	Out-scat.	1.18301	1.03652	1.04665	29	32	27
			In-scat., P0 flux wgt	1.18296	1.03647	1.04658	24	28	21
			In-scat., PL flux wgt	div.	div.	div.	div.	div.	div.
P2-P3	P0, P1, P2	P3	Out-scat.	1.18279	1.03629	1.04635	10	10	−1
			In-scat., P0 flux wgt	1.18276	1.03626	1.04632	8	8	−5
			In-scat., PL flux wgt	div.	div.	div.	div.	div.	div.

*) diverged

Table 3 K-effective in small core configuration (H_2O reflector, BWR)

Method	Treatment of scattering matrix		Evaluation of	K-infinity			Difference (pcm)		
	Full	Diagonal	diagonal element	4.1 wt% UO2	2 wt% UO2	12 wt% MOX	4.1 wt% UO2	2 wt% UO2	12 wt% MOX
P0	P0	—	—	1.26566	1.11566	1.11203	4237	4434	3656
P1	P0, P1	—	—	1.21319	1.06744	1.07125	−84	−80	−146
P2	P0, P1, P2	—	—	1.21434	1.06841	1.07300	10	11	18
P3	P0, P1, P2, P3	—	—	1.21421	1.06830	1.07282	0	0	0
Out-scatter-tr	P0	—	Out-scat.	1.20764	1.06239	1.06783	−541	−552	−464
In-scatter-tr			In-scat., P0 flux wgt	1.22352	1.07635	1.08251	766	754	904
In-scatter-tr			In-scat., PL flux wgt	div.*)	div.	div.	div.	div.	div.
P0-P1	P0	P1	Out-scat.	1.20205	1.05748	1.06047	−1002	−1013	−1151
			In-scat., P0 flux wgt	1.22034	1.07356	1.07726	504	493	415
			In-scat., PL flux wgt	div.	div.	div.	div.	div.	div.
P0-P2	P0	P1, P2	Out-scat.	1.20368	1.05889	1.06275	−868	−880	−938
			In-scat., P0 flux wgt	1.22160	1.07466	1.07920	608	596	595
			In-scat., PL flux wgt	div.	div.	div.	div.	div.	div.
P0-P3	P0	P1, P2, P3	Out-scat.	1.20369	1.05890	1.06258	−867	−879	−954
			In-scat., P0 flux wgt	1.22155	1.07462	1.07896	604	592	572
			In-scat., PL flux wgt	div.	div.	div.	div.	div.	div.
P1-P2	P0, P1	P2	Out-scat.	1.21457	1.06865	1.07330	29	33	45
			In-scat., P0 flux wgt	1.21451	1.06860	1.07324	24	28	39
			In-scat., PL flux wgt	1.21463	1.06871	1.07336	35	38	51
P1-P3	P0, P1	P2, P3	Out-scat.	1.21457	1.06865	1.07313	30	33	29
			In-scat., P0 flux wgt	1.21447	1.06856	1.07300	21	25	17
			In-scat., PL flux wgt	div.	div.	div.	div.	div.	div.
P2-P3	P0, P1, P2	P3	Out-scat.	1.21435	1.06842	1.07283	11	11	1
			In-scat., P0 flux wgt	1.21430	1.06837	1.07277	7	7	−5
			In-scat., PL flux wgt	div.	div.	div.	div.	div.	div.

*) diverged

Table 4 K-effective in small core configuration (SS reflector, AWR)

Method	Treatment of scattering matrix		Evaluation of	K-infinity			Difference (pcm)		
	Full	Diagonal	diagonal element	4.1 wt% UO2	2 wt% UO2	12 wt% MOX	4.1 wt% UO2	2 wt% UO2	12 wt% MOX
P0	P0	—	—	1.26594	1.11062	1.11639	1912	2295	1441
P1	P0, P1	—	—	1.24154	1.08518	1.09926	−52	−49	−115
P2	P0, P1, P2	—	—	1.24232	1.08582	1.10072	10	10	17
P3	P0, P1, P2, P3	—	—	1.24219	1.08571	1.10054	0	0	0
Out-scatter-tr	P0	—	Out-scat.	1.24239	1.08568	1.10254	16	−3	182
In-scatter-tr			In-scat., P0 flux wgt	1.24553	1.08884	1.10498	268	288	404
In-scatter-tr			In-scat., PL flux wgt	1.24399	1.08717	1.10418	145	134	331
P0-P1	P0	P1	Out-scat.	1.23944	1.08307	1.09718	−221	−243	−305
			In-scat., P0 flux wgt	1.24275	1.08641	1.09968	45	64	−78
			In-scat., PL flux wgt	1.24118	1.08469	1.09890	−81	−94	−149
P0-P2	P0	P1, P2	Out-scat.	1.24051	1.08402	1.09900	−135	−156	−140
			In-scat., P0 flux wgt	1.24377	1.08731	1.10146	127	147	84
			In-scat., PL flux wgt	1.24221	1.08560	1.10069	1	−10	14
P0-P3	P0	P1, P2, P3	Out-scat.	1.24050	1.08401	1.09878	−136	−157	−159
			In-scat., P0 flux wgt	1.24375	1.08728	1.10122	125	145	63
			In-scat., PL flux wgt	div.*)	div.	div.	div.	div.	div.
P1-P2	P0, P1	P2	Out-scat.	1.24257	1.08609	1.10105	30	34	47
			In-scat., P0 flux wgt	1.24256	1.08608	1.10104	30	34	46
			In-scat., PL flux wgt	1.24257	1.08609	1.10106	31	35	47
P1-P3	P0, P1	P2, P3	Out-scat.	1.24256	1.08608	1.10084	30	34	27
			In-scat., P0 flux wgt	1.24254	1.08605	1.10081	28	32	25
			In-scat., PL flux wgt	div.	div.	div.	div.	div.	div.
P2-P3	P0, P1, P2	P3	Out-scat.	1.24231	1.08582	1.10051	9	10	−3
			In-scat., P0 flux wgt	1.24229	1.08580	1.10049	8	8	−4
			In-scat., PL flux wgt	div.	div.	div.	div.	div.	div.

*) diverged

Table 2 indicates that the P0 result significantly overestimates the k-effective since no anisotropic scattering (especially forward peaked scattering of hydrogen) is taken into account in the P0 result. The P1 result slightly underestimates the k-effective and its magnitude depends on the fuel type. In contrast, the P2 result well reproduces the reference results regardless of the fuel type. Therefore, the consideration of the P2 anisotropic scattering is sufficient in the present small core configurations of the present study, as described in the cell calculation.

In the transport corrected cross sections, the definition of the transport cross section has a large impact on the calculation results. The out-scatter approximation gives a negative bias, though the in-scatter approximation gives a positive bias and the difference between the out-scatter and in-scatter approximations almost reaches 1,000 pcm. The in-scatter approximation with the PL flux moment (current) weighted cross section shows numerical instability (*i.e.*, divergence). In order to clarify these observations, the transport corrected cross section and its ratio to the total cross section for H_2O are shown in **Figs. 3** and **4**, respectively. From Figs. 3 and 4, the out-scatter and in-scatter approximations show discrepancy in the fast energy region, especially higher than 1 keV. Since the in-scatter approximation gives a larger transport corrected cross section in the fast energy region, it gives a higher k-effective than the out-scatter approximation due to reduced neutron leakage in the high-energy region. In the in-scatter approximation with PL flux moment (current) weight, the transport corrected cross section becomes negative in a particular energy group, *e.g.*, 5×10^5 eV. This would be a reason for numerical instability. Figure 4 indicates that the negative transport cross section is also obtained at ~7 eV, but this negative transport cross section is not used in the calculation. (It should be noted that only the out-scatter approximation is used for the energy range lower than 1 keV.) The cause of the negative transport corrected cross section will be discussed later. Note that the validity of the transport corrected cross section in the transport calculation will be discussed in more detail in the next section.

The P0-P1 treatment underestimates k-effective when the out-scatter approximation is used to evaluate the diagonal element. In contrast, the in-scatter approximation overestimates k-effective. The reason for these under- and over-predictions would be the same as that for the transport corrected cross sections, as discussed above. Actually, the transport corrected cross sections defined by Eqs. (2), (4), and (5) are evaluated by subtracting the diagonal elements of the P1 scattering matrix obtained using formulae (6)–(8) from the total cross section.

The discrepancy of the P1-P2 results is smaller and more stable than that of P1, *i.e.*, independent of the fuel type. Therefore, the P1-P2 treatment can be recommended as a simplified treatment of anisotropic scattering, as discussed in the cell calculation. This approach has advantages over the conventional P2 treatment since the P2 scattering matrix

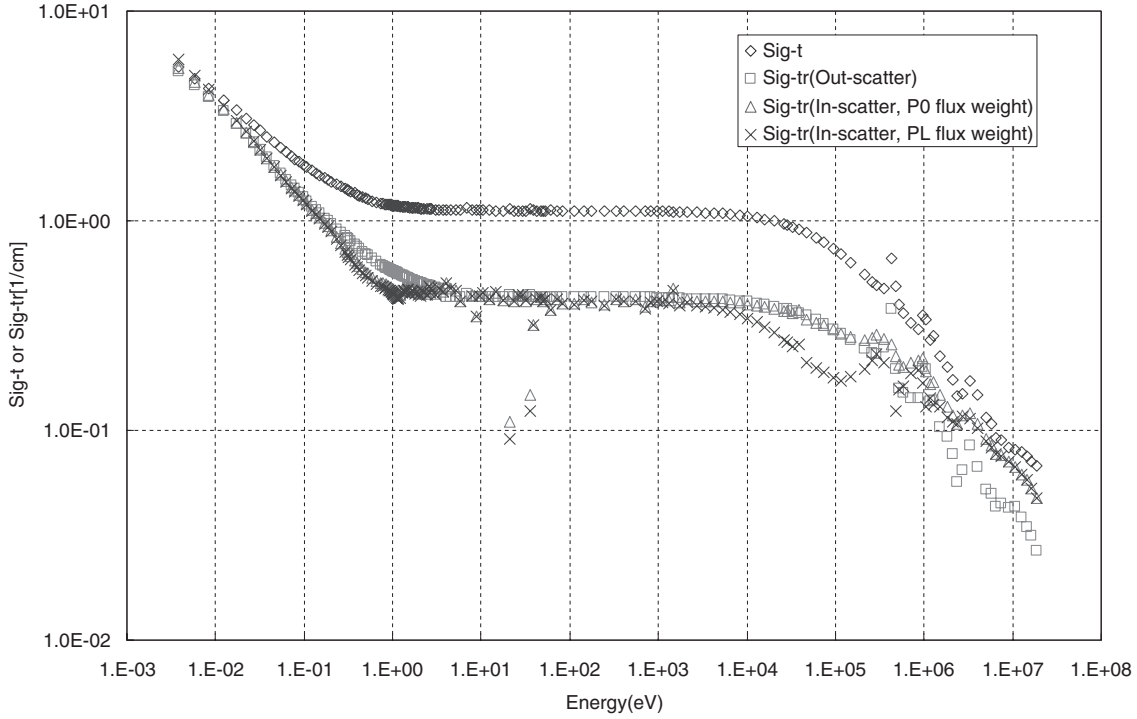

Fig. 3 Total and transport corrected cross sections for H_2O

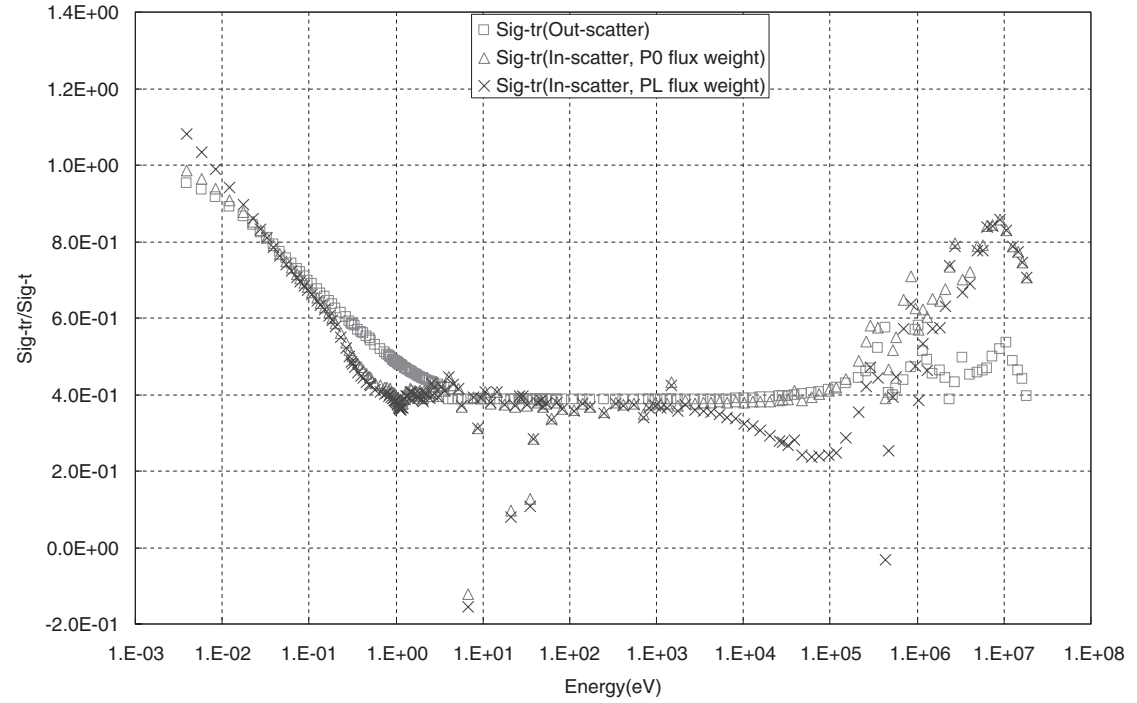

Fig. 4 Ratio of transport corrected cross section to total cross section for H_2O

can be treated as the diagonal element. The P1-P2 and P1-P3 treatments show similar results; thus, the treatment of the P3 component would not be necessary.

Numerical instability is observed in some cases when the PL flux moment is used for the weighting factor to evaluate the diagonal element. In order to clarify the cause of such instability, the diagonal element of the scattering matrix for water (H_2O) and the flux moments used for the weighting factor are shown in **Figs. 5–8**. Diagonal elements obtained by the three different methods (out-scatter, in-scatter with scalar flux, in-scatter with PL flux moment) are shown in these figures. It should be noted that only the out-scatter approximation is applied to the energy range lower than 1 keV. The P1 diagonal element shows similar trends regardless of

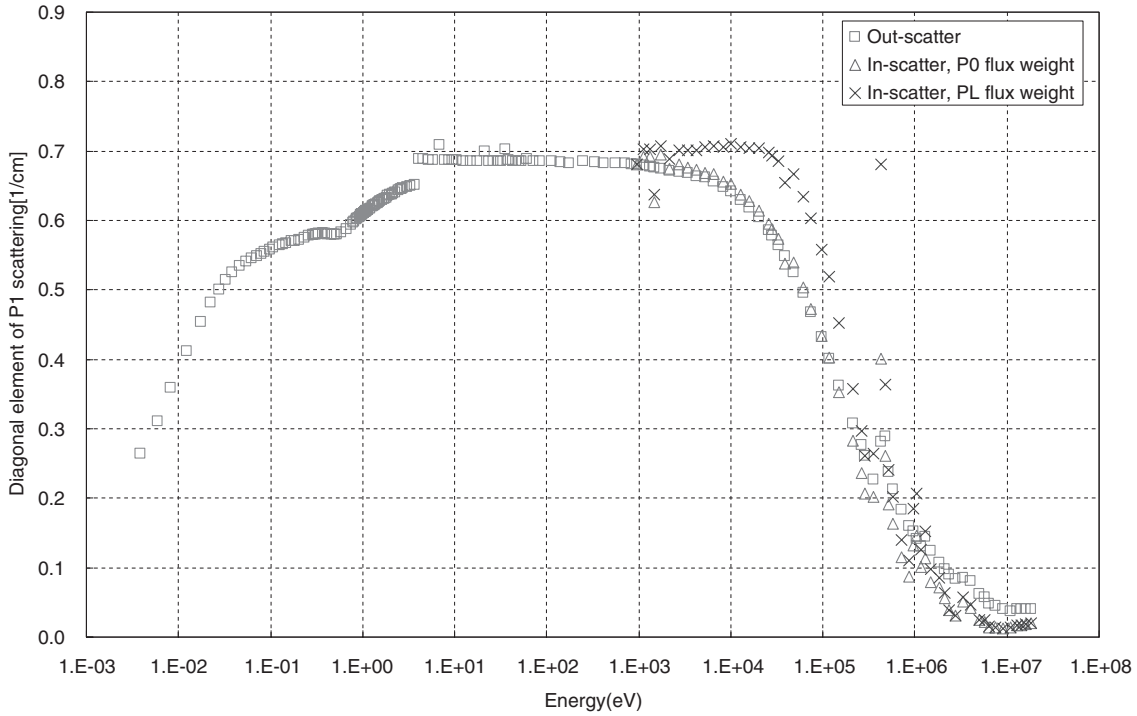

Fig. 5 Diagonal element of P1 scattering matrix for H_2O

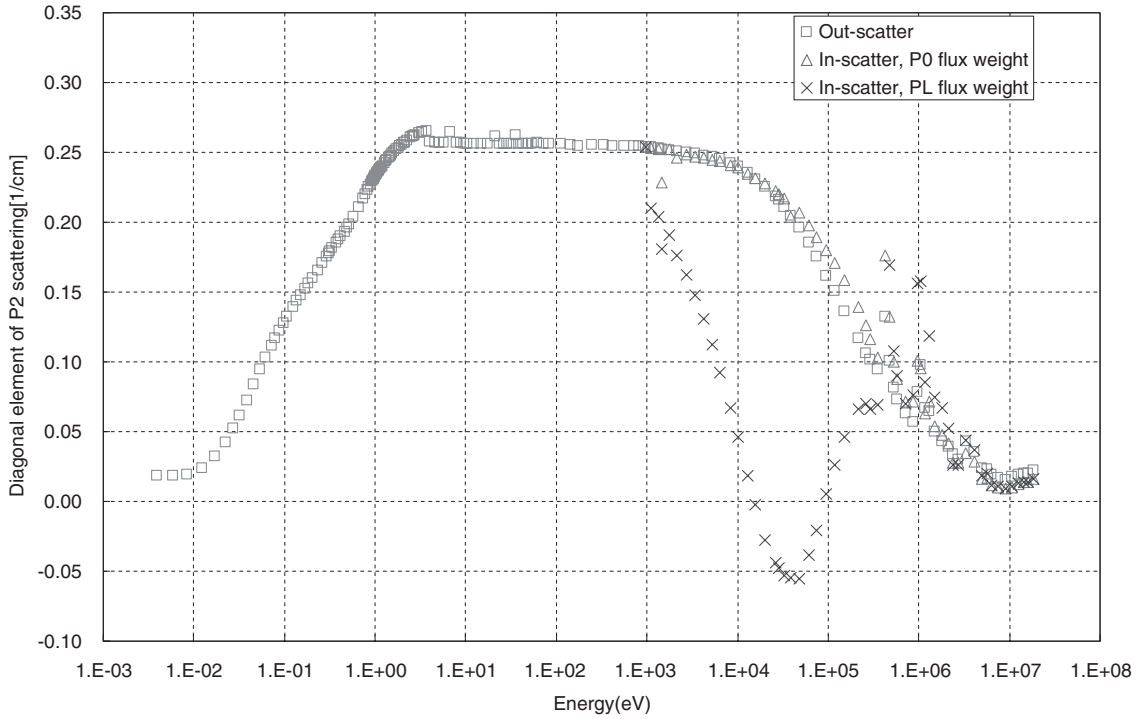

Fig. 6 Diagonal element of P2 scattering matrix for H_2O

the evaluation method used, as shown in Fig. 3. In the case of the P2 element, the in-scatter approximation with the PL flux moment weight shows a different behavior, as shown in Fig. 6. Figure 7 indicates that the diagonal element obtained by the in-scatter approximation with the PL flux moment gives a significantly large negative value for the P3 component of around 10^5 eV.

This observation can be explained by the shape of the approximated P3 flux moment shown in Fig. 8. Since the PL flux moments are evaluated using $\phi_{l,g} \approx \phi_{0,g}/(\Sigma_{t,g})^l$, and $\Sigma_{t,g}$ is smaller for the higher energy range, flux shape shows a "harder spectrum" for higher flux moments, as shown in Fig. 8. The diagonal element of a scattering matrix is evaluated using $\Sigma_{sl,g\to g} \approx \sum_{g'} \Sigma_{sl,g'\to g}\phi_{l,g'}/\phi_{l,g}$. At around

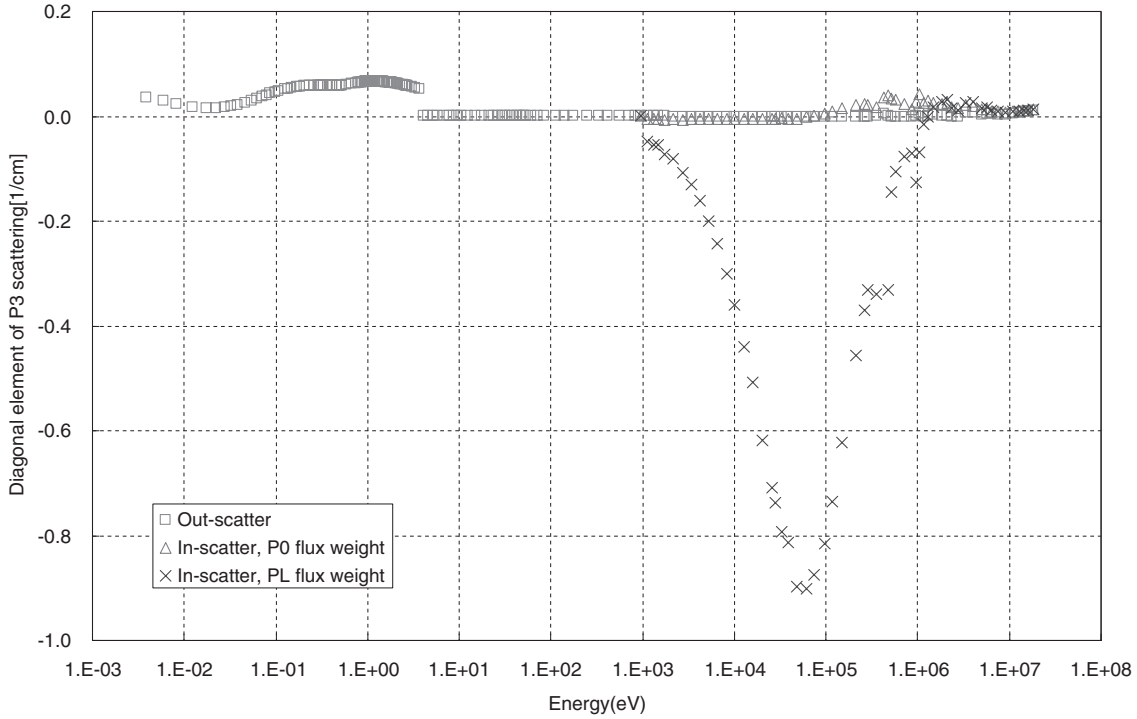

Fig. 7 Diagonal element of P3 scattering matrix for H_2O

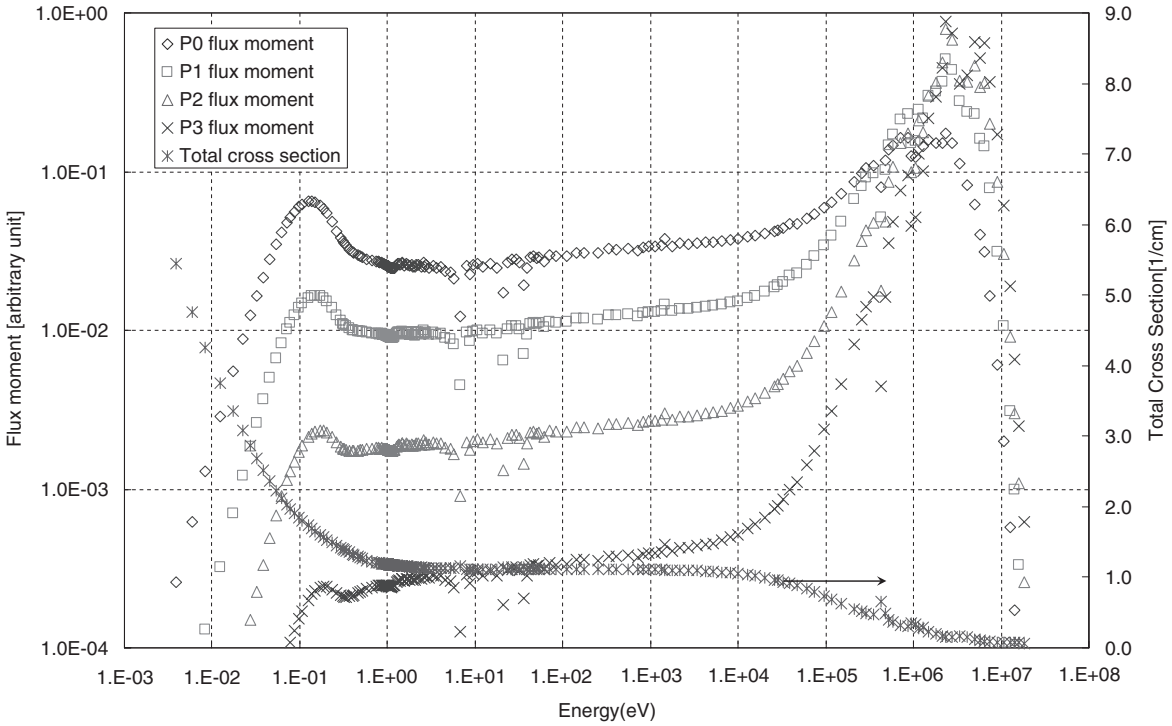

Fig. 8 Approximate flux moments and total cross section for H_2O

10^5 eV, though the slowing down source of the PL component ($\sum_{g'} \Sigma_{sl,g'\to g}\phi_{l,g'}$) is large due to the shape of PL flux moment, the denominator ($\phi_{l,g}$) rapidly decreases. Consequently, the evaluated diagonal element ($\Sigma_{sl,g\to g}$) increases. The above large diagonal element of an anisotropic scattering matrix ($\Sigma_{sl,g\to g}$) would be the cause of another numerical instability in addition to the negative transport cross section. Note that the diagonal element of the P3 scattering matrix evaluated by the above procedure can be negative since the scattering matrix for the P3 component contains not only positive values but also negative values. In other words, the summation of the in-scatter P3 source ($\sum_{g'} \Sigma_{s3,g'\to g}\phi_{3,g'}$) may be negative since the components of the scattering matrix ($\Sigma_{s3,g'\to g}$) may be negative. Therefore, from the practical

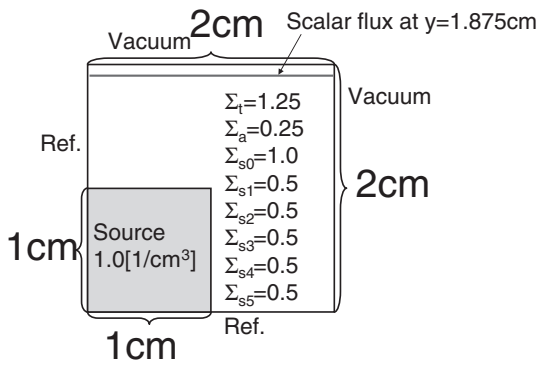

Fig. 9 Geometry of one-group fixed source benchmark problem

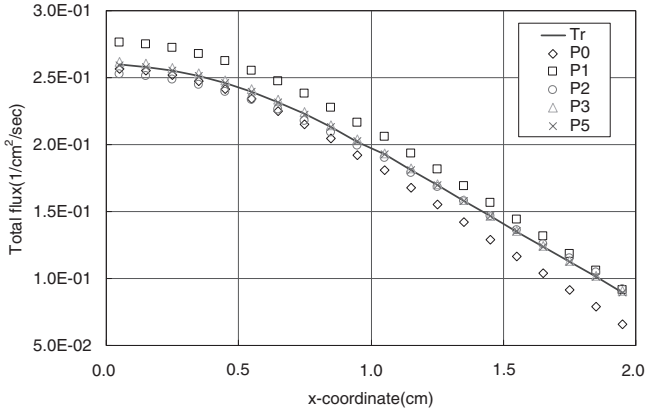

Fig. 10 Calculation result for one-group fixed source benchmark problem

point of view, the PL flux moment weight especially for the higher order anisotropic component may not be favorable.

The negative transport corrected cross section observed in the in-scatter approximation with PL flux weight is also explained by the above discussion. The total cross section of H_2O increases at around 5×10^5 eV due to the resonance of ^{16}O; thus, the current evaluated using $\phi_{1,g} \approx \phi_{0,g}/\Sigma_{t,g}$ decreases. Therefore, the diagonal element obtained using $\Sigma_{s1,g\to g} \approx \sum_{g'} \Sigma_{s1,g'\to g}\phi_{1,g'}/\phi_{1,g}$ increases in this energy range. Consequently, the transport corrected cross section obtained using $\Sigma_{tr,g} = \Sigma_{t,g} - \Sigma_{s1,g\to g}$ becomes negative.

Tables 2–4 indicate that the calculation results also depend on the type of reflector. The water reflector (Table 3) gives the largest diversity of discrepancy among the three types of reflector since the anisotropic scattering cross section for hydrogen is larger than the medium weight elements (*e.g.*, Fe, Ni, Cr) used in SS. The effect of anisotropic scattering treatment is smallest in the SS bulk reflector used in APWR due to a smaller anisotropic scattering component.

The above discussion suggests that a full anisotropic scattering matrix up to the P1 component would be necessary in the present approach to accurately evaluate neutronics properties in high-leakage systems. However, the P2 component can be approximated using the diagonal element. Therefore, reductions in memory storage and computation time can be expected while maintaining the calculation accuracy. Another important observation is that the transport corrected cross section with the in-scatter approximation overestimates k-effective. The latter issue will be discussed in detail in the next section.

IV. Validity of the Transport Corrected Cross Section in Transport Calculation

In order to discuss the validity of the transport corrected cross section in transport calculations, a simple benchmark problem,[12] which is a one-group fixed-source problem with anisotropic scattering, is analyzed. Calculation geometry and cross sections are shown in **Fig. 9**. Calculations are carried out using the AEGIS code with the following discretization parameters.

- Azimuthal angles: 64
- Polar angles: 2 (Tabuchi-Yamamoto's quadrature set)
- Ray trace width: 0.02 cm
- Sub-mesh division for flat flux region: 0.2 cm × 0.2 cm

In the present calculation, the anisotropic scattering components up to P5 are taken into account. The total (scalar) flux distribution at $y = 1.875$ cm is evaluated with the following treatment of anisotropic scattering.

- P0: neglect P1–P5 anisotropic scattering components
- P1: neglect P2–P5 anisotropic scattering components
- P2: neglect P3–P5 anisotropic scattering components
- P3: neglect P4–P5 anisotropic scattering components
- P5: reference
- Sig-tr (TR): transport corrected cross section ($\Sigma_{tr} = \Sigma_t - \Sigma_{s1}$) is used and isotropic scattering is assumed. Note that $\Sigma_{s0} - \Sigma_{s1}$ is used for the P0 scattering cross section approximation in order to adjust cross section balance. The P2-P5 anisotropic scattering cross sections are neglected.

Since the present benchmark problem is a one-group problem, there is no ambiguity on the transport corrected cross section, as discussed in section II. Furthermore, the magnitude of the higher order anisotropic scattering is set to be the same in order to clarify the discussion on the physical meaning of the transport corrected cross section. A detailed discussion on this point will appear later in this section.

The calculation result is shown in **Fig. 10**. Figure 10 clearly indicates that the transport calculation results with the higher order anisotropic scattering converge that with the transport corrected cross section. This result can be explained as follows:

Equation (3) is a one-group transport equation in one-dimensional geometry:

$$\mu \frac{d\psi(x,\mu)}{dx} + \Sigma_t(x)\psi(x,\mu) = \sum_{l=0}^{\infty} \frac{2l+1}{4\pi} P_l(\mu)\Sigma_{sl}(x)\phi_l(x) + S(x), \quad (17)$$

where

μ: direction cosine,
$\psi(x,\mu)$: angular flux at position x and direction μ,
$P_l(\mu)$: Legendre polynomial,
$\Sigma_{sl}(x)$: l-th order anisotropic scattering cross section,
$\phi_l(x)$: l-th order of angular flux moment, and
$S(x)$: (isotropic) external source.

When the anisotropic scattering cross sections ($\Sigma_{s1}(x)$, $\Sigma_{s2}(x), \ldots$) are identical, Eq. (17) can be written as follows:

$$\mu \frac{d\psi(x,\mu)}{dx} + \Sigma_t(x)\psi(x,\mu) = \Sigma_{sL}(x) \sum_{l=0}^{\infty} \frac{2l+1}{4\pi} P_l(\mu)\phi_l(x) + \frac{1}{4\pi}(\Sigma_{s0}(x) - \Sigma_{sL}(x))\phi_0(x) + S(x), \quad (18)$$

where

$\Sigma_{sL}(x)$: anisotropic scattering, $\Sigma_{s1}(x) = \Sigma_{s2}(x) = \Sigma_{s3}(x) = \ldots = \Sigma_{sL}(x)$.

From the definition of the angular flux moment,

$$\psi(x,\mu) = \sum_{l=0}^{\infty} \frac{2l+1}{4\pi} P_l(\mu)\phi_l(x) \quad (19)$$

Substituting Eq. (19) into Eq. (18), we obtain

$$\mu \frac{d\psi(x,\mu)}{dx} + \Sigma_t(x)\psi(x,\mu) = \Sigma_{sL}(x)\psi(x,\mu) + \frac{1}{4\pi}(\Sigma_{s0}(x) - \Sigma_{sL}(x))\phi_0(x) + S(x). \quad (20)$$

Finally, Eq. (20) can be written as

$$\mu \frac{d\psi(x,\mu)}{dx} + \Sigma_{tr}(x)\psi(x,\mu) = \frac{1}{4\pi}(\Sigma_{s0}(x) - \Sigma_{sL}(x))\phi_0(x) + S(x), \quad (21)$$

where

$$\Sigma_{tr}(x) = \Sigma_{tr}(x) - \Sigma_{sL}(x).$$

The above derivation clarifies the observation found in Fig. 10, *i.e.*, the consideration of the infinite order of anisotropic scatterings with identical values is mathematically equivalent to the utilization of the transport corrected cross section and isotropic scattering. In other words, the utilization of the transport corrected cross section is always equivalent to the consideration of the infinite order of anisotropic scatterings with identical values.

The transport corrected cross section is usually used to consider the first-order (linearly) anisotropic scattering. However, the above discussion reveals the following fact. When the transport corrected cross section is used in a transport calculation, not only the first-order anisotropic scattering cross section but also the higher (> first) order anisotropic scattering cross sections are always implicitly taken into account.[8] In general, when the P2 or higher order anisotropic scattering cross section is taken into account, the estimated neutron leakage tends to decrease. Therefore, a higher order anisotropic scattering calculation tends to give a higher k-effective than the P1 anisotropic scattering calculation. Since the utilization of the transport corrected cross section in a transport calculation implicitly considers the higher order anisotropic scattering, the transport corrected cross section tends to give a higher k-effective. The above explanation indicates the root cause of the overestimation of k-effective in small cores when the transport corrected cross section (in-scatter approximation) is used. In other words, when the transport corrected cross section is "accurately" estimated using

$$\Sigma_{tr,g} = \Sigma_{t,g} - \frac{\sum_{g'} \Sigma_{s1,g' \to g}\phi_{0,g'}}{\phi_{0,g}},$$

k-effective would be overestimated. It is empirically known that the transport corrected cross section evaluated by the in-scatter approximation results in the overestimation of k-effective in a small core (*e.g.*, critical assembly) when it is used in a transport calculation.[10] The above discussion indicates the reason for the overestimation of k-effective with the transport corrected cross section obtained by the in-scatter approximation. It should be noted that the sensitivity of the transport corrected cross section would be much smaller in large configurations, such as LWR cores.

The transport cross section with the out-scatter approximation results in the underestimation of k-effective. From Fig. 4, the transport corrected cross section with the out-scatter approximation is smaller than that with the in-scatter approximation in the fast energy range. The discrepancy comes from the fact that the neutron energy balance used in the derivation of Eq. (5) is no more valid in the high-energy region. Consequently, the out-scatter transport cross section tends to overestimate neutron leakage from the core; thus, the k-effective is "fortunately" underestimated. The underestimated k-effective values obtained using the out-scatter transport corrected cross section are approximately 1,000, 1,300, and 250 pcm for PWRs, BWRs, and APWRs, respectively. Due to the cancellation of errors (*i.e.*, the overestimation of k-effective due to the implicit consideration of the higher order anisotropic scattering and the underestimation of k-effective due to the smaller transport cross section in the fast energy range), the transport corrected cross section with the out-scatter approximation gives a smaller discrepancy from the reference value. The present discussion suggests the reason why the transport corrected cross section with the out-scatter approximation tends to show a higher accuracy than the in-scatter approximation in a transport calculation.

V. Conclusion

Various approximate treatments of anisotropic scattering are tested in LWR pin cells and small cores using various fuel types and reflectors. Calculation results indicate that the anisotropic scattering matrixes up to the P1 component would be explicitly included for the precise analysis of small cores. However, the P2 anisotropic scattering effects are effectively captured by the in-scatter or out-scattering approximation for the P2 scattering matrixes. The P3 component has small impact on the calculation results for the configurations in the present study; thus, it could be truncated. Consequently, the P1-P2 treatment (full scattering matrixes for P0 and P1, the diagonal approximation for P2) is sufficient in the present study. Since the P1-P2 approximation can reduce memory storage requirement for the scattering matrix compared with the explicit P2 treatment, this approximation will be computationally efficient.

When the in-scatter approximation with the PL flux moment weight is used to evaluate the diagonal element of an anisotropic scattering matrix, numerical instability is observed in some cases. Therefore, from the practical point of view, total (P0) flux would be a desirable weighting factor for evaluating the diagonal element of an anisotropic scattering matrix in the in-scatter approximation.

In addition to the investigation of simplified treatments of the anisotropic scattering, the physical meaning of the transport corrected cross section utilized in a transport calculation is discussed through a simple one-group fixed-source benchmark problem. The discussion suggests that the transport corrected cross section implicitly takes into account the higher order anisotropic scattering that is not explicitly considered in the definition of the transport corrected cross section. Since the consideration of the higher order anisotropic scattering tends to reduce neutron leakage, k-effective is generally overestimated with transport corrected cross sections. This would be a possible reason for the overestimation of k-effective in a transport calculation with the in-scatter transport cross section. The out-scatter approximation gives better results due to the cancellation of errors.

In the conventional design calculation of LWRs, the transport corrected cross section with isotropic scattering is usually used. Therefore, a better derivation of the transport corrected cross section would be favorable for the affinity with the current design framework. Such effort is desirable and an improvement in the transport corrected cross section is still an open problem.

References

1) P. T. Petkov, T. Takeda, "Transport calculations of MOX and UO2 pin cells by the method of Characteristics," *J. Nucl. Sci. Technol.*, **35**, 12 (1998).
2) T. Ushio, T. Takeda, M. Mori, "Neutron anisotropic scattering effect in heterogeneous cell calculations of light water reactors," *J. Nucl. Sci. Technol.*, **40**, 464 (2003).
3) J. Rhodes, K. Smith, D. Lee, "CASMO-5 development and applications," *Proc. PHYSOR2006, ANS Topical Meeting on Reactor Physics*, Vancouver, Canada, Sep. 10–14, 2006, B144 (2006).
4) T. Takeda, T. Okamoto, A. Inoue, S. Kosaka, H. Ikeda, "Effect of anisotropic scattering in neutronics analysis of BWR assembly," *Ann. Nucl. Energy*, **33**, 1315 (2006).
5) D. Knott, V. W. Mills, E. Wehlage, "Description and validation of the lattice physics code LANCER02," *Proc. Mathematics and Computation, Supercomputing, Reactor Physics and Nuclear and Biological Applications*, Palais de Papes, Avignon, France, Sep. 12–15, 2005, American Nuclear Society, (2005). [CD-ROM]
6) N. Sugimura, T. Ushio, A. Yamamoto *et al.* "Development of advanced neutronics design system of next generation, AEGIS," *Proc. Mathematics and Computation, Supercomputing, Reactor Physics and Nuclear and Biological Applications*, Palais des Papes, Avignon, France, Sep. 12–15, 2005 (2005). [CD-ROM]
7) C. V. Gaudard, A. Santamarina, A. Sargeni *et al.*, "Qualification of APOLLO2 BWR calculation scheme on the BASALA mock-up," *Proc. PHYSOR2006, ANS Topical Meeting on Reactor Physics*, Vancouver, Canada, Sep. 10–14, 2006, B2124 (2006).
8) G. I. Bell, G. E. Hansen, H. A. Sandmeier, "Multitable treatments of anisotropic scattering in SN multigroup transport calculations," *Nucl. Sci. Eng.*, **28**, 376 (1967).
9) G. Chiba, "Effect of neutron anisotropic scattering and treatment of angular dependency of neutron flux in effective cross section on criticality in fast reactor analysis," *Trans. At. Energy Soc. Jpn.*, **3**, 200 (2004), [in Japanese].
10) A. Yamamoto, S. Shiroya, K. Kanda, "Transport and anisotropic scattering effects on effective multiplication factor in small cores of the KUCA," *Annual Reports of the Research Reactor Institute*, **22**, 78 (1989).
11) R. E. MacFarlane, D. W. Muir, *The NJOY Nuclear Data Processing System Version 91*, LA-12740-M, p.VIII-17 (1994).
12) R. Roy, "Anisotropic scattering for integral transport codes. Part 2 cyclic tracking and its application to XY lattices," *Ann. Nucl. Energy*, **18**, 511 (1991).
13) N. Sugimura, A. Yamamoto, T. Ushio, M. Mori, M. Tabuchi, T. Endo, "Neutron transport models of AEGIS: An advanced next-generation neutronics design system," *Nucl. Sci. Eng.*, **155**, 276 (2007).
14) A. Yamamoto, K. Tada, N. Sugimura, T. Ushio, M. Mori, "Generation of cross section library for lattice physics code, AEGIS," *Proc. PHYSOR2006, ANS Topical Meeting on Reactor Physics*, Vancouver, Canada, Sep. 10–14, 2006 (2006). [CD-ROM]
15) A. Yamamoto, M. Tabuchi, N. Sugimura, T. Ushio, M. Mori, "Derivation of optimum polar angle quadrature set for the method of characteristics based on approximation error of the bickley function," *J. Nucl. Sci. Technol.*, **44**, 129 (2007).